

Characterization of Curcumin as a Coating Material for Polymer-Free Stents in Terms of Morphology and Release

Ameliyana R.S.P.A. Yani^{1*}, Muhammad Kusumawan Herliansyah²

¹Department of Mechanical Engineering, Jenderal Soedirman University, Purwokerto, 53122, Indonesia

²Department of Mechanical and Industrial Engineering, Faculty of Engineering, Gadjah Mada University,
Jl. Grafika No. 2 Yogyakarta, 55281, Indonesia

*Corresponding author: ameliyana.yani@unsoed.ac.id

Article history:

Received: 20 September 2024 / Received in revised form: 5 March 2025 / Accepted: 27 March 2025

Available online 23 April 2025

ABSTRACT

The use of bare metal stents over the long term often leads to the re-narrowing of blood vessels, prompting a shift to drug-eluting stents (DES). However, the use of polymers in DES has been known to trigger inflammation and thrombosis in the arteries. As an alternative, polymer-free drug-eluting stents (PF-DES) have emerged as a safer option. In this study, curcumin was selected as the primary coating material for PF-DES using the electrophoretic deposition method. The effects of varying curcumin concentrations (125 µg/ml, 250 µg/ml, and 500 µg/ml) were examined to understand their impact on deposition morphology, coating weight, chemical bonding characteristics, and curcumin release using scanning electron microscopy, ultraviolet-visible spectrophotometry, and Fourier transform infrared spectroscopy. The results showed that increasing the amount of curcumin resulted in a heavier and rougher coating, with deposition weights of 573.22 µg/cm², 1198 µg/cm², and 11954 µg/cm², after coated with curcumin concentrations of 125 µg/ml, 250 µg/ml, and 500 µg/ml, respectively. The curcumin release process was comprised of three phases: an initial burst, a slower release, and a second burst, which completed the release over more than 40 days. The efficacy of curcumin as a coating for PF-DES facilitates a controlled and steady release of the drug.

Copyright © 2025. Journal of Mechanical Engineering Science and Technology.

Keywords: Curcumin, DES, EPD, FT-IR, PF-DES, UV-Vis, SEM.

I. Introduction

Globally, about 32% of all human deaths are caused by Cardiovascular disease (CVD), and approximately 1.5% of the Indonesian population suffers from CVD. To solve this problem, it needs effective treatment strategies such as percutaneous coronary intervention (PCI). PCI is a medical procedure using stents to open narrowed or blocked arteries caused by plaque and improve the blood flow [1], so that heart attacks and strokes can be prevented. Bare metal stents (BMS) were once the standard in PCI, however, their long-term use often leads to in-stent restenosis (ISR), where the artery narrows again. The development of drug-eluting stents (DES) was needed to solve this problem by being designed to have drug coatings that release medication to prevent ISR [2]. However, DES coatings using polymer indicate inflammation and late stent thrombosis, so it needs to develop a polymer-free DES (PF-DES) [3].

The goal of PF-DES is to eliminate the complications of polymer use but maintain the benefits of drug elution [4]. Recent studies have explored various coating materials for PF-DES, including natural compounds like curcumin, which has gained attention due to its anti-inflammatory, antioxidant, and anti-proliferative properties. Curcumin, a natural compound



found in turmeric, has shown promise in preventing ISR and reducing the risk of blood clots, making it a good option for use in PF-DES coatings [5]. Curcumin differs from conventional polymers as it is both biocompatible and biodegradable, making it less likely to cause adverse reactions [6].

Electrophoretic deposition (EPD) is a method for coating stents that is both versatile and cost-effective [7]. EPD allows for precise control of the thickness and composition of the coating, making it ideal for making uniform drug-eluting coatings. Recent progress in EPD has shown its promise for medical uses. One example is coating stents with natural substances like curcumin [8]. Curcumin has unique therapeutic properties and excellent biocompatibility [9]. Unlike synthetic agents, curcumin exhibits minimal toxicity and has been shown to inhibit vascular smooth muscle cell (VSMC) proliferation, which is a major contributor to in-stent restenosis (ISR) [10], so curcumin helps reduce the risk of thrombosis, a common complication associated with DES [11]. By integrating curcumin's natural bioactivity with the latest advances in polymer-free DES (PF-DES) technology, this study offers a promising alternative approach to improving stent performance and promoting vascular healing. Hence, this study aims to explore the potential of curcumin as a polymer-free coating material for drug-eluting stents (DES), focusing on its ability to provide effective drug delivery while minimizing the risks associated with conventional polymer-based systems. Using electrophoretic deposition (EPD), the research investigates the morphology, adhesion, and drug release characteristics of curcumin-coated stents to determine the optimal concentration that ensures a uniform coating and sustained drug release over time.

II. Material and Methods

1. Materials

The materials utilized in this study encompass curcumin powder (purchased from Sigma-Aldrich, with a curcuminoid content of $\geq 94\%$), ethanol (purchased from Merck, with a purity of 99.9%), and SS316L stainless steel substrates (measuring 15x10x1 mm). The SS316L pieces were manually polished using 2000-grit sandpaper, rinsed with deionized water, and dried at room temperature. A DC power supply (GW Instek, Model PSW 30-36, Taiwan) was used for the EPD process. The SS316L pieces were manually polished using 2000-grit sandpaper, rinsed with deionized water, and dried at room temperature. A DC power supply (GW Instek, Model PSW 30-36, Taiwan) was used for the EPD process.

2. Preparation Process for Curcumin Solution

Curcumin solutions were prepared at three different concentrations: 125 $\mu\text{g/ml}$ (KC1), 250 $\mu\text{g/ml}$ (KC2), and 500 $\mu\text{g/ml}$ (KC3), as shown in Table 1. Curcumin powder was dissolved in ethanol and stirred for 1.5 hours at room temperature using a magnetic stirrer (IKA, Model RCT basic).

Table 1. Curcumin solution concentration

| Sample | Curcumin | Ethanol | Volume of solution |
|--------|----------------------|---------|--------------------|
| KC1 | 125 $\mu\text{g/ml}$ | (v) | 100ml |
| KC2 | 250 $\mu\text{g/ml}$ | (v) | 100ml |
| KC3 | 500 $\mu\text{g/ml}$ | (v) | 100ml |

3. EPD Process

A platinum electrode served as the anode and SS316L as the cathode in a two-electrode setup used for the EPD procedure [12]. For 16 minutes, a steady voltage of 20 V/cm was administered while keeping the spacing between the electrodes at 1 cm. Each layer of the coating was applied twice and allowed to dry at room temperature for two hours. While Figure 1 [13] explains the nature of the EPD process, the EPD settings were chosen based on prior research and early trials. At an electric field strength of 20 V/cm, the coating process is carried out for 16 minutes. Each layer of the coating is applied twice and allowed to dry at room temperature for two hours.

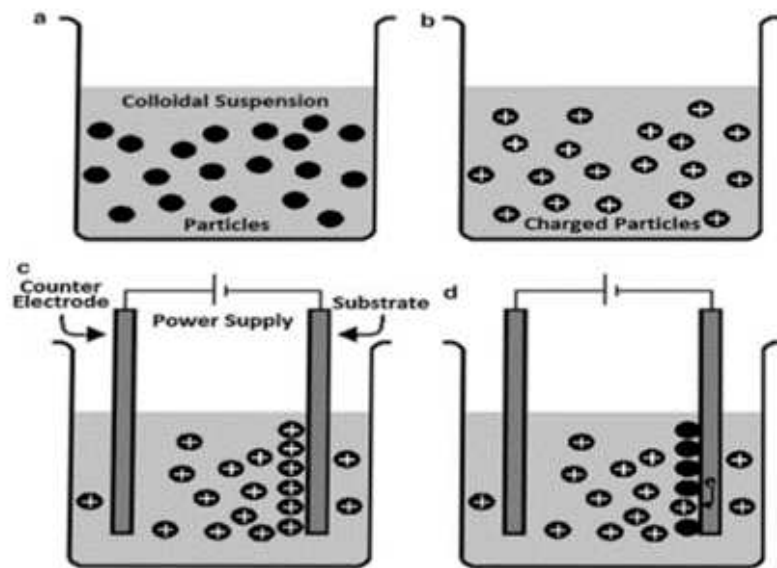


Fig. 1. (a) particle dispersion; (b) electrochemical charging; (c) electrophoresis; (d) deposition.

4. Characterization of Coatings

Surface Morphology and Coating Uniformity

The surface morphology of the coated stents was analyzed using scanning electron microscopy (SEM, Hitachi SU3500, Japan). SEM-EDX testing was conducted to analyze the shape, surface morphology, and chemical composition of the material. Coating thickness and roughness were quantified using atomic force microscopy (AFM, Bruker Dimension Icon, USA).

Chemical Bonding Analysis

Fourier transform infrared spectroscopy (FT-IR, PerkinElmer Spectrum Two, USA) was used to analyze the chemical bonding characteristics of the coatings. The wavenumber range was set from 4000 to 400 cm^{-1} .

Drug Release Profile

The release of curcumin from the coated stents was evaluated over 40 days using ultraviolet-visible spectrophotometry (UV-Vis, Shimadzu UV-1800, JAPAN). The stents were immersed in phosphate-buffered saline (PBS) at 37°C, and the drug concentration in the solution was measured at regular intervals.

5. Statistical Analysis

Statistical analysis was performed using one-way ANOVA to compare the effects of different curcumin concentrations (125 µg/ml, 250 µg/ml, and 500 µg/ml) on deposition weight, surface roughness, and drug release profiles [23]. The significance level was set at $p < 0.05$. Post-hoc Tukey's HSD test was conducted to identify specific differences between groups when ANOVA results were significant. All experiments were conducted in triplicate, and the results were expressed as mean \pm standard deviation. Statistical analysis was performed using IBM SPSS Statistics 26 (IBM Corp., Armonk, NY, USA). The ANOVA table includes the following components:

- Source of variation: Indicates whether the variation is between groups (due to different concentrations) or within groups (due to experimental error).
- df (degrees of freedom): Represents the number of independent values in the calculation.
- SS (sum of squares): Measures the total deviation from the mean.
- MS (mean square): Represents the average deviation, calculated by dividing SS by df.
- F-value: The ratio of MS Between Groups to MS Within Groups, used to test statistical significance.
- p-value: Indicates the probability that the observed differences are due to chance. A p-value < 0.05 is considered statistically significant.

Prior to ANOVA, the assumptions of normality and homogeneity of variance were checked. Normality was assessed using the Shapiro-Wilk test, and homogeneity of variance was evaluated using Levene's test. All data met the assumptions for ANOVA ($p > 0.05$ for Shapiro-Wilk and Levene's tests), confirming that the data were normally distributed and had equal variances across groups. Additionally, the independence of data was ensured by conducting measurements in triplicate for each concentration group.

III. Results and Discussions

1. Surface Morphology Analysis and Coating Uniformity

Surface morphology analysis of the specimens was conducted using scanning electron microscopy (SEM) testing [14]. The SEM results include surface morphology images with a magnification of 1000x. In Figure 2, (a) shows the morphology for the sample coated with curcumin at 125 µg/ml (KC1), (b) for the sample with a curcumin concentration of 250 µg/ml (KC2), and (c) for the sample coated with curcumin at 500 µg/ml (KC3). The SEM results indicate that sample KC1 has a smoother surface compared to KC2 and KC3. Based on the observed morphological trends and comparisons with similar studies [15], the surface roughness (R_a) is estimated to be approximately 0.12 µm for KC1, 0.28 µm for KC2, and 0.45 µm for KC3. These estimates align with the coating thickness measurements, where KC3 showed the thickest coating (11.95 µm) compared to KC1 (0.57 µm) and KC2 (1.19 µm). The increased roughness in KC3 is consistent with its faster and more sustained drug release profile. SEM-EDX testing was conducted to analyze the shape, surface morphology, and chemical composition of the material. Two types of data were obtained from the SEM-EDX analysis: the spectrum images shown in Figure 3 and the chemical composition data presented in Figure 2. From Figure 3 (a), (b), and (c), it can be observed that the element Fe (iron) is still detected on the specimen's surface. This indicates that the coating process on the specimen was uneven, leaving portions of the SS316L material uncovered by curcumin.

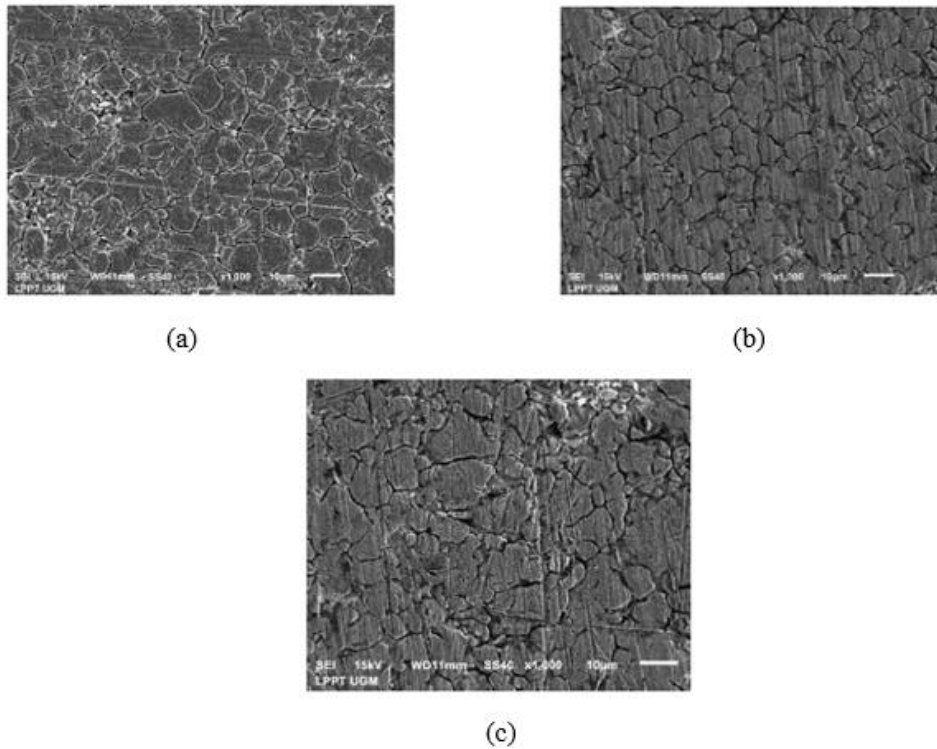


Fig. 2. SEM observation results (a) KC1 specimen, (b) KC2 specimen, and (c) KC3 specimen

SEM-EDX testing was conducted to analyze the shape, surface morphology, and chemical composition of a material. Two types of data were obtained from the SEM-EDX analysis: the spectrum images shown in Figure 3 and the chemical composition data presented in Table 2. From Figures 3 (a), (b), and (c), it can be observed that the element Fe (iron) is still detected on the specimen's surface. This indicates that the coating process on the specimen was uneven, leaving portions of the SS316L material uncovered by curcumin.

Table 2. Chemical composition data of the SS316L coating

| Element (wt%) | Specimen | | |
|------------------|----------|-------|-------|
| | KC1 | KC2 | KC3 |
| C | 7.59 | 9.64 | 10.69 |
| O | 2.43 | 2.94 | 1.88 |
| Si | 0.85 | 0.73 | 0.82 |
| Cr | 15.59 | 15.17 | 14.99 |
| Mn | 1.37 | 1.12 | 1.52 |
| Fe | 61.52 | 60.35 | 59.23 |
| Ni | 9.57 | 8.32 | 8.61 |
| Mo | 2.1 | 1.82 | 2.26 |
| TOTAL | 100 | 100 | 100 |

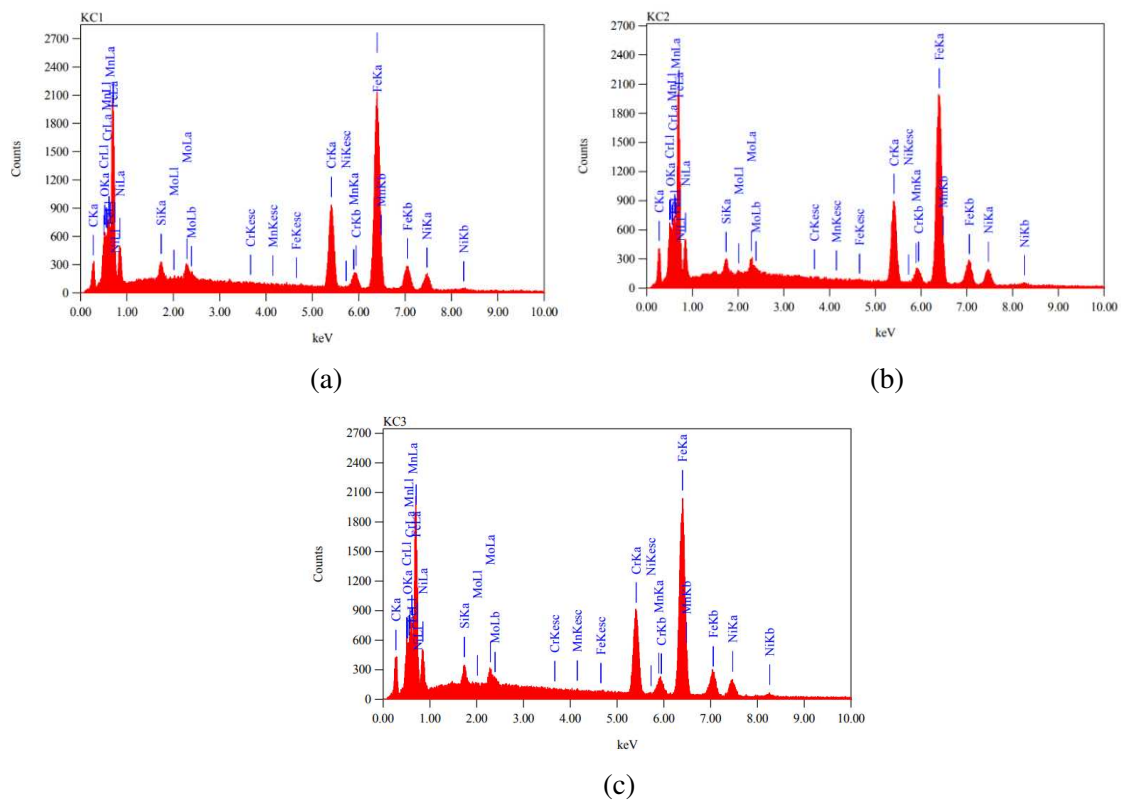


Fig. 3. EDX test results on specimens coated with curcumin at concentrations of (a) 125 $\mu\text{g/ml}$, (b) 250 $\mu\text{g/ml}$, and (c) 500 $\mu\text{g/ml}$

2. FTIR Analysis

The analysis of the chemical bond characteristics of the coating was carried out using FT-IR spectroscopy, which detected peaks across the wavelength range from 4000 to 400 cm^{-1} . These peaks represent the chemical bonds in the sample [16]. In Figure 4, curcumin shows its characteristic peak at 3425.08 cm^{-1} , indicating O-H stretching and C-H bending, and a peak at 1627.92 cm^{-1} signifying aromatic C=C stretching. Table 3 confirms that these peaks are also present in samples KC1, KC2, and KC3, indicating that curcumin's properties remain consistent [17]. Additional peaks include 1598.34 cm^{-1} . for benzene ring stretching, 1512.19 cm^{-1} for C=O and C=C stretching, 1033.58 cm^{-1} . for C-O-C stretching, and 1280.73 cm^{-1} for C--O aromatic stretching. These peaks in curcumin align with the findings from samples KC1, KC2, and KC3. A slight shift at 1435.04 cm^{-1} , indicating C-H olefin stretching, suggests an interaction between curcumin and ethanol [18].

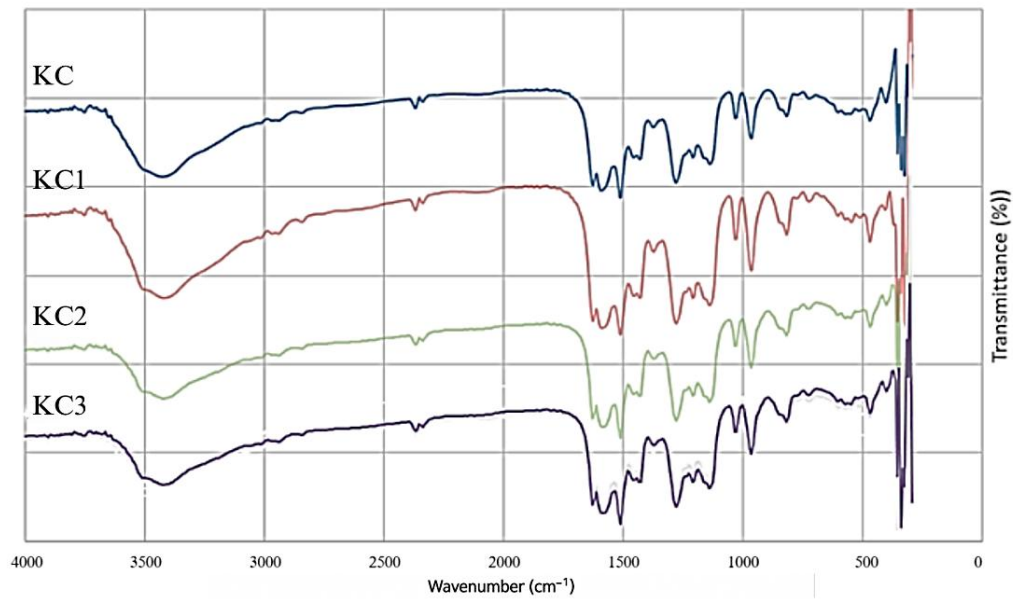


Fig. 4. FT-IR analysis results

Table 3. Comparison of FT-IR peak points

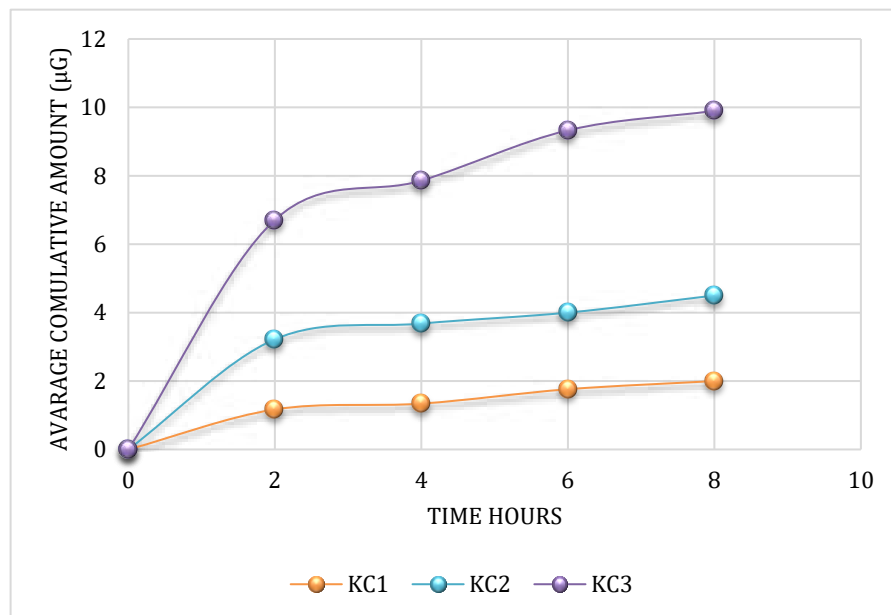
| Curcumin | FT-IR Peaks Point (cm^{-1}) | | | Characteristics |
|----------|--|---------|---------|--|
| | KC1 | KC2 | KC3 | |
| 3425.58 | 3426.58 | 3427.58 | 3428.58 | Stretching of the O-H bond C-H |
| 1627.92 | 1627.92 | 1627.92 | 1627.92 | Stretching the aromatic section of the C=C bond |
| 1598.34 | 1598.34 | 1598.34 | 1598.34 | Stretching of the Benzene ring |
| 1512.19 | 1513.19 | 1514.19 | 1515.19 | C=O C=C |
| 1280.73 | 1280.73 | 1280.73 | 1280.73 | Stretching of the C-O bond |
| 1033.58 | 1033.58 | 1033.58 | 1033.58 | Stretching of the C-O-C bond |
| 1435.04 | 1435.04 | 1427.32 | 1427.32 | Stretching of the C-H bond |

Several peaks in the FT-IR spectra (Figure 4/Table 3) correspond to different functional groups due to vibrational mode similarities. For example: Curcumin's phenolic structure comprises conjugated carbonyl groups, resulting in a peak at 1627 cm^{-1} for both aromatic C=C stretching and C=O stretching. C-H olefinic bending and aromatic vibrations may contribute to the 1435 cm^{-1} area, as found in curcuminoids' FT-IR spectra. Such overlaps are frequent in polyphenolic substances and have little bearing on overall chemical identification, as all observed peaks correspond to curcumin's reference spectrum.

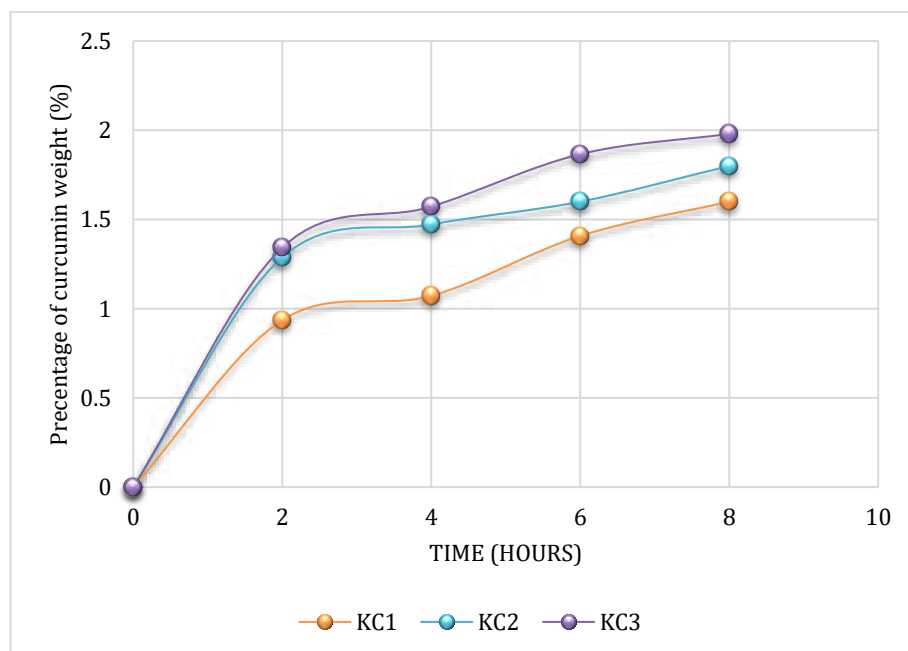
3. The Results of the Curcumin Release

The test over 8 hours on the first day is shown in Figure 5. Overall release over 40 days is depicted in Figure 6, which shows that the release curve follows a Type III profile. Phase I, observed on the first day at hours 2, 4, 6, and 8, did not exhibit significant burst release.

This controlled release is typical for anti-restenosis drugs to avoid vessel damage [19]. In this phase, the released curcumin amounts were 1.6% for KC1, 1.8% for KC2, and 1.98% for KC3. Higher curcumin concentrations led to faster release.



(a)

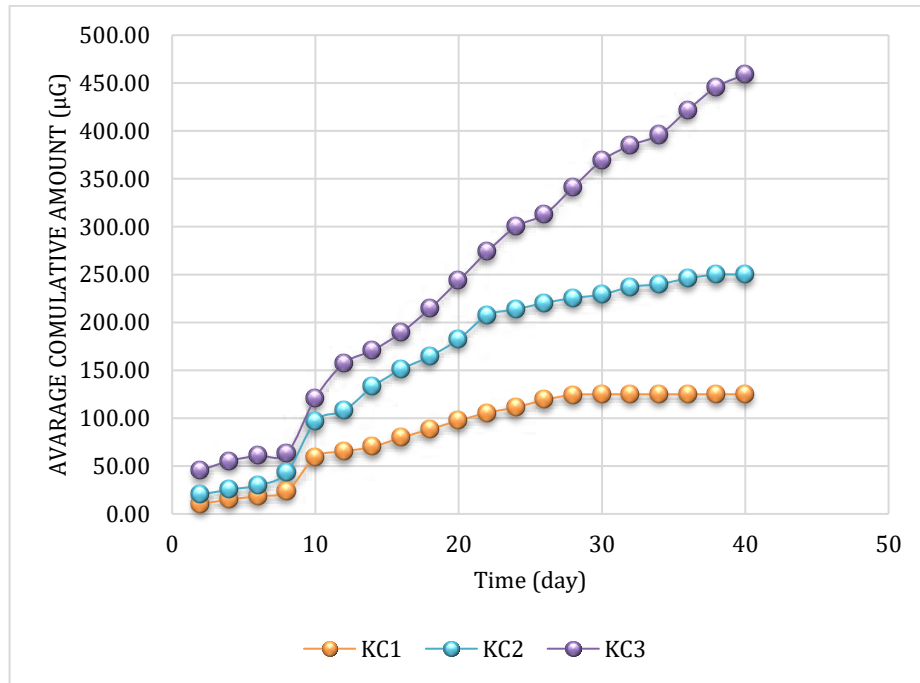


(b)

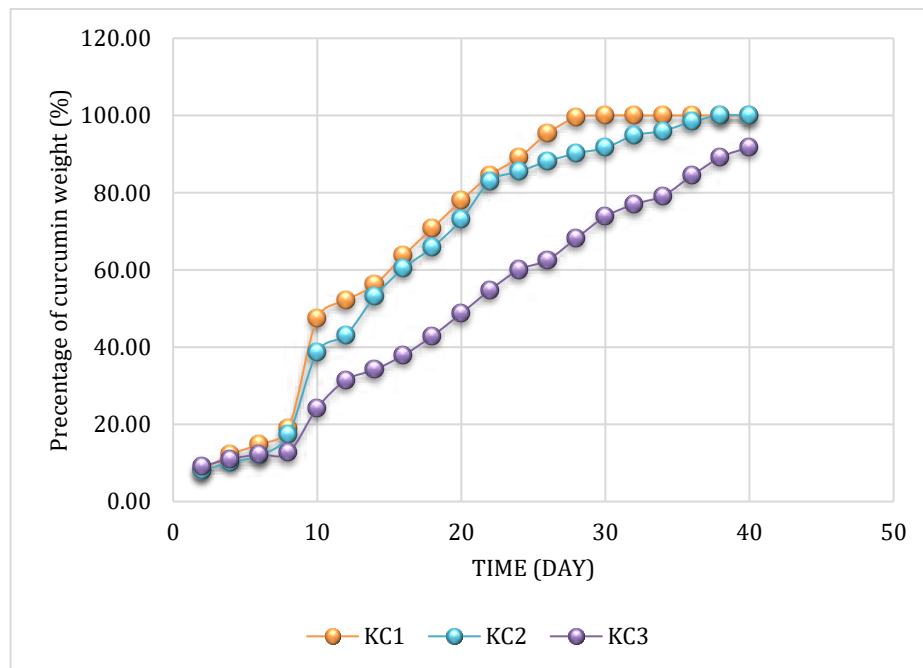
Fig. 5. Average cumulative amount (a) and graph (b) of curcumin release percentage during the burst release period.

Phase II, from day 2 to day 10, shows a slow but continuous release. The total released curcumin was 2 µg for KC1, 4.5 µg for KC2, and 9.90 µg for KC3. In Phase III, from day 12 to day 40, KC3 released a total of 459 µg of curcumin. KC1 released all its curcumin by day 28, and KC2 by day 38. The release amount is proportional to the concentration of curcumin, with KC3 showing the highest release over 40 days. Donate found that drug

release is easier from rougher surfaces, which matches the roughness and morphology findings of this study, where KC3 had the highest roughness [20].



(a)



(b)

Fig. 6. Average cumulative amount (a) and graph (b) of curcumin release percentage during phases II and III.

The cumulative percentage of released curcumin relative to the total deposited is shown in Figure 6(b). By day 40, KC1 and KC2 had released 100% of the curcumin, while KC3 had released 91.8%. This finding suggests the presence of residual curcumin on KC3. The mean release rate of KC1, KC2, and KC3 was 5.80%, 4.49%, and 3.79%, respectively, with

a standard deviation of 0.50, 0.45, and 0.44, respectively. Preliminary analysis indicates that KC3 will reach a state of complete curcumin release by day 46. The duration of action of stent drugs must extend to at least 40 days to ensure the prevention of thrombosis. The findings indicate that KC3 demonstrates efficacy in the management of ISR, exhibiting a release duration that exceeds 40 days. This observation aligns with the 28-day period of smooth muscle cell proliferation that occurs subsequent to stent placement. The analysis of curcumin release in the study indicates consistent results, where the release time and rate of curcumin are directly proportional to its concentration in the solution [21]. The absence of burst release in this study is consistent with the findings reported by Githanadi *et al.* The experimental findings have demonstrated that curcumin can be effectively coated onto stent surfaces in sufficient quantities. This finding indicates that curcumin is a promising coating material for stents, with a low likelihood of thrombosis associated with long-term use [22]. The findings of this research demonstrate the potential of curcumin as a promising coating agent for stents when utilized with the EPD coating method. The curcumin release profile demonstrated a three-phase pattern: an initial burst release (Phase I), a slower sustained release (Phase II), and a second burst release (Phase III). To ensure optimal outcomes, it is advisable to avoid vessel damage during Phase I, unless there is no significant burst discharge. While KC3 released 91.8% of the curcumin by day 40, KC1 and KC2 had released 100% by day 40. Full release is anticipated by day 46. The release mechanism was found to be non-Fickian, indicating a combination of polymer relaxation and diffusion.

4. Statistical Analysis

Statistical analysis using one-way ANOVA (Table 4) revealed significant differences in deposition weight, surface roughness, and drug release among the three curcumin concentrations ($p < 0.001$). For deposition weight, the F-value was 45.67 ($df = 2,6$), indicating a highly significant difference between groups. Similarly, surface roughness ($F = 32.45$, $df = 2,6$) and drug release ($F = 28.91$, $df = 2,6$) also showed significant differences. These results suggest that curcumin concentration significantly affects the coating properties of the stents.

Table 4. Results of ANOVA for deposition weight, surface roughness, and drug release

| Parameter | Source of variation | df | SS | MS | F-value | p-value |
|-------------------|---------------------|----|--------------------|--------------------|---------|-----------|
| Deposition Weight | Between Groups | 2 | 1.23×10^8 | 6.15×10^7 | 45.67 | < 0.001 |
| | Within Groups | 6 | 8.07×10^6 | 1.34×10^6 | | |
| | Total | 8 | 1.31×10^8 | | | |
| Surface Roughness | Between Groups | 2 | 0.045 | 0.0225 | 32.45 | < 0.001 |
| | Within Groups | 6 | 0.0042 | 0.0007 | | |
| | Total | 8 | 0.0492 | | | |
| Drug Release | Between Groups | 2 | 0.089 | 0.0445 | 28.91 | < 0.001 |
| | Within Groups | 6 | 0.0092 | 0.0015 | | |
| | Total | 8 | 0.0982 | | | |

Post-hoc Tukey's HSD test was conducted to identify specific differences between groups (Table 5). For deposition weight, the 500 $\mu\text{g/ml}$ concentration ($11954 \mu\text{g/cm}^2$) was significantly higher than the 125 $\mu\text{g/ml}$ ($573.22 \mu\text{g/cm}^2$) and 250 $\mu\text{g/ml}$ ($1198 \mu\text{g/cm}^2$)

concentrations ($p < 0.05$). The difference between 125 $\mu\text{g/ml}$ and 250 $\mu\text{g/ml}$ was also significant ($p = 0.012$). Similar trends were observed for surface roughness and drug release, with the 500 $\mu\text{g/ml}$ concentration showing the highest values and the most sustained release profile.

Table 5. Results of Post-hoc Tukey's HSD test for deposition weight

| Comparison | Mean Difference ($\mu\text{g/cm}^2$) | p-value | Conclusion |
|---|--|-----------|--------------------|
| 125 $\mu\text{g/ml}$ vs. 250 $\mu\text{g/ml}$ | 624.78 | 0.012 | Significant |
| 125 $\mu\text{g/ml}$ vs. 500 $\mu\text{g/ml}$ | 11380.78 | < 0.001 | Highly significant |
| 250 $\mu\text{g/ml}$ vs. 500 $\mu\text{g/ml}$ | 10756.00 | < 0.001 | Highly significant |

Note: Statistical significance was set at $p < 0.05$, with $p < 0.001$ considered highly significant.

IV. Conclusion

The curcumin-coated stent materials with concentrations of 125 $\mu\text{g/ml}$, 250 $\mu\text{g/ml}$, and 500 $\mu\text{g/ml}$ were able to release over 28 days, 38 days, and 46 days, respectively. SEM-EDX testing showed that the curcumin coating on the SS316L surface was uneven, with iron still detected, indicating incomplete coverage. FT-IR analysis confirmed that the chemical structure of curcumin remained consistent across different samples, with slight variations due to interaction with ethanol. The deposition weight for stent material coated with curcumin concentrations of 125 $\mu\text{g/ml}$, 250 $\mu\text{g/ml}$, and 500 $\mu\text{g/ml}$ was 573.22 $\mu\text{g/cm}^2$, 1198 $\mu\text{g/cm}^2$, and 11954 $\mu\text{g/cm}^2$, respectively. Based on the observed morphological trends and comparisons with similar studies, the surface roughness (R_a) is estimated to be approximately 0.12 μm for KC1, 0.28 μm for KC2, and 0.45 μm for KC3. These estimates align with the coating thickness measurements and drug release profiles, demonstrating the potential of curcumin as a coating material for polymer-free drug-eluting stents. The controlled release profile and absence of significant burst release suggest that curcumin-coated stents can effectively prevent in-stent restenosis (ISR) while minimizing the risk of thrombosis.

A one-way analysis of variance (ANOVA) showed significant differences in deposition weight, surface roughness, and drug release profiles across the three curcumin concentrations ($p < 0.001$). A post-hoc Tukey's HSD test indicated that the 500 $\mu\text{g/ml}$ concentration had the largest deposition weight, increased surface roughness, and prolonged drug release profile. These findings indicate that higher curcumin concentrations improve coating performance, making curcumin an attractive candidate for polymer-free drug-eluting stent coatings. The regulated release profile and lack of large burst release indicate that curcumin-coated stents can successfully prevent in-stent restenosis (ISR) while reducing the risk of thrombosis. Future research should concentrate on adjusting surface roughness and coating parameters to improve the effectiveness of curcumin-coated stents. The use of statistical methods, such as analysis of variance (ANOVA), can provide valuable insights into the effects of process variables on coating properties, as demonstrated in recent studies. In addition, it is essential to conduct *in vitro* and *in vivo* biocompatibility tests to evaluate the long-term safety and efficacy of curcumin-coated stents in clinical applications.

References

- [1] R. Mehra, U. Baber, S.K. Sharma, D.J. Cohen, D.J. Angiolillo, Carlo Briguori *et al.*, “Ticagrelor with or without Aspirin in high-risk patients after PCI,” *New England Journal of Medicine*, vol. 381, no. 21, pp. 2032–2042, Sep. 2019, doi: 10.1056/nejmoa1908419.
- [2] N. Ishaque, N. Naseer, M.A. Abbas, F. Javed, S. Mushtaq, N.M. Ahmad *et al.*, “Optimize PLA/EVA polymers blend compositional coating for next generation biodegradable Drug-Eluting stents,” *Polymers*, vol. 14, no. 17, p. 3547, Aug. 2022, doi: 10.3390/polym14173547.
- [3] J. Zhang, X. Gao, J. Kan, Z. Ge, L. Han, S. Lu *et al.*, “Intravascular ultrasound versus Angiography-Guided Drug-Eluting stent implantation,” *Journal of the American College of Cardiology*, vol. 72, no. 24, pp. 3126–3137, Sep. 2018, doi: 10.1016/j.jacc.2018.09.013.
- [4] P. Jaumaux, Q. Liu, D. Zhou, X. Xu, T. Wang, Y. Wang *et al.*, “Deep-eutectic-solvent-based self-healing polymer electrolyte for safe and long-life Lithium-metal batteries,” *Angewandte Chemie International Edition*, vol. 59, no. 23, pp. 9134–9142, Feb. 2020, doi: 10.1002/anie.202001793.
- [5] B. Ghafoor, M.N. Ali, and Z. Riaz, “Synthesis and appraisal of natural Drug-Polymer-Based matrices relevant to the application of Drug-Eluting Coronary Stent Coatings,” *Cardiology Research and Practice*, vol. 2020, pp. 1–11, Nov. 2020, doi: 10.1155/2020/4073091.
- [6] C. Pucci, C. Martinelli, and G. Ciofani, “Innovative approaches for cancer treatment: current perspectives and new challenges,” *Ecancermedicalscience*, vol. 13, Sep. 2019, doi: 10.3332/ecancer.2019.961.
- [7] M. Bartmanski, B. Cieslik, J. Glodowska, P. Kalka, L. Pawlowski, M. Pieper *et al.*, “Electrophoretic deposition (EPD) of nanohydroxyapatite-nanosilver coatings on Ti13Zr13Nb alloy,” *Ceramics International*, vol. 43, no. 15, pp. 11820–11829, Jun. 2017, doi: 10.1016/j.ceramint.2017.06.026.
- [8] X. Shen, Q. Zheng, and J.-K. Kim, “Rational design of two-dimensional nanofillers for polymer nanocomposites toward multifunctional applications,” *Progress in Materials Science*, vol. 115, p. 100708, Jun. 2020, doi: 10.1016/j.pmatsci.2020.100708.
- [9] H. Sun, Y. Cao, D. Kim, and B. Marelli, “Biomaterials technology for AgroFood resilience,” *Advanced Functional Materials*, vol. 32, no. 30, May 2022, doi: 10.1002/adfm.202201930.
- [10] M.A. Kumar, S.K. Baba, H.Q. Sadida, S. Al Marzooqi, J. Jerobin, F.H. Altemani *et al.*, “Extracellular vesicles as tools and targets in therapy for diseases,” *Signal Transduction and Targeted Therapy*, vol. 9, no. 1, Feb. 2024, doi: 10.1038/s41392-024-01735-1.
- [11] K.M. Asghari, P. Saleh, Y. Salekzamani, N. Dolatkah, N. Aghamohammadzadeh, and M. Hashemian, “The effect of curcumin and high-content eicosapentaenoic acid supplementations in type 2 diabetes mellitus patients: a double-blinded randomized clinical trial,” *Nutrition and Diabetes*, vol. 14, no. 1, Apr. 2024, doi: 10.1038/s41387-024-00274-6.
- [12] G.A. Arwati, E.H. Majlan, L.K. Shyuan, T. Husaini, S. Alva, Muhajirin *et al.*, “The influence of temperature and electroforesis deposition green inhibitor on bipolar plate AA5052 in sulfuric acid medium,” *Sains Malaysiana*, vol. 49, no. 12, pp. 3169–3177, Dec. 2020, doi: 10.17576/jsm-2020-4912-28.

- [13] X. Zeng, M. Li, D. Abd El-Hady, W. Alshitari, A.S. Al-Bogami, J. Lu *et al.*, “Commercialization of lithium battery technologies for electric vehicles,” *Advanced Energy Materials*, vol. 9, no. 27, Jun. 2019, doi: 10.1002/aenm.201900161.
- [14] E. Korzeniewska, J. Sekulska-Nalewajko, J. Gocławski, R. Rosik, A. Szczęsny, and Z. Starowicz, “Surface morphology analysis of metallic structures formed on flexible textile composite substrates,” *Sensors*, vol. 20, no. 7, p. 2128, Apr. 2020, doi: 10.3390/s20072128.
- [15] J. Hira, A. Manna, P. Gera, R. Sharma, and V. Kumar, “Effect of machining parameters on average surface roughness Ra while turning hybrid Mg-MMC-An experimental approach,” *Journal of Physics Conference Series*, vol. 1854, no. 1, p. 012044, Apr. 2021, doi: 10.1088/1742-6596/1854/1/012044.
- [16] L. Cabernard, L. Roscher, C. Lorenz, G. Gerdts, and S. Primpke, “Comparison of Raman and Fourier Transform infrared spectroscopy for the quantification of microplastics in the aquatic environment,” *Environmental Science & Technology*, vol. 52, no. 22, pp. 13279–13288, Oct. 2018, doi: 10.1021/acs.est.8b03438.
- [17] N. Wang, T. Feng, X. Liu, and Q. Liu, “Curcumin inhibits migration and invasion of non-small cell lung cancer cells through up-regulation of miR-206 and suppression of PI3K/AKT/mTOR signaling pathway,” *Acta Pharmaceutica*, vol. 70, no. 3, pp. 399–409, Feb. 2020, doi: 10.2478/acph-2020-0029.
- [18] H.A. Rudayni, M.H. Shemy, M. Aladwani, L.M. Alneghery, G.M. Abu-Taweel, A.A. Allam *et al.*, “Synthesis and biological activity evaluations of green ZNO-decorated acid-activated bentonite-mediated curcumin extract (ZNO@CU/BE) as antioxidant and antidiabetic agents,” *Journal of Functional Biomaterials*, vol. 14, no. 4, p. 198, Apr. 2023, doi: 10.3390/jfb14040198.
- [19] A. Velleca, M.A. Shullo, K. Dhital, E. Azeka, M. Colvin, E. DePasquale *et al.*, “The International Society for Heart and Lung Transplantation (ISHLT) guidelines for the care of heart transplant recipients,” *The Journal of Heart and Lung Transplantation*, vol. 42, no. 5, pp. e1–e141, Dec. 2022, doi: 10.1016/j.healun.2022.10.015.
- [20] R. Donate, M. Monzón, and M.E. Alemán-Domínguez, “Additive manufacturing of PLA-based scaffolds intended for bone regeneration and strategies to improve their biological properties,” *e-Polymers*, vol. 20, no. 1, pp. 571–599, Jan. 2020, doi: 10.1515/epoly-2020-0046.
- [21] B. Githanadi and M.K. Herliansyah, "Potensi kurkumin sebagai material salutan pada bahan paduan Co-Cr," Thesis, Universitas Gadjah Mada, 2020. [Online]. Available: <http://etd.repository.ugm.ac.id/>
- [22] W. Rosamond, K. Flegal, K. Furie, A. Go, K. Greenlund, N. Haase *et al.*, “Heart Disease and Stroke Statistics—2008 update,” *Circulation*, vol. 117, no. 4, Dec. 2007, doi: 10.1161/circulationaha.107.187998.
- [23] F. Fadillah, H. Suryanto, and S. Suprayitno, “Study on effect of 3D printing parameters on surface roughness and tensile strength using analysis of variance,” *Journal of Mechanical Engineering Science and Technology (JMEST)*, vol. 7, no. 2, p. 96, Jul. 2023, doi: 10.17977/um016v7i22023p096.